Inorganic Chemistry

FORUM ARTICLE

pubs.acs.org/IC

Synthesis, Characterization, and Multielectron Reduction Chemistry of Uranium Supported by Redox-Active α-Diimine Ligands

Steven J. Kraft,[†] Ursula J. Williams,[‡] Scott R. Daly,[§] Eric J. Schelter,[‡] Stosh A. Kozimor,[§] Kevin S. Boland,[§] James M. Kikkawa,[⊥] William P. Forrest,[†] Christin N. Christensen,[§] Daniel E. Schwarz,[§] Phillip E. Fanwick,[†] David L. Clark,[§] Steve D. Conradson,[§] and Suzanne C. Bart*[,†]

[†]H. C. Brown Laboratory, Department of Chemistry, Purdue University, West Lafayette, Indiana 47907, United States

[‡]P. Roy and Diana T. Vagelos Laboratories, Department of Chemistry, University of Pennsylvania, Philadelphia, Pennsylvania 19104, United States

[§]Los Alamos National Laboratory, Los Alamos, New Mexico 87545, United States

[⊥]Department of Physics & Astronomy, University of Pennsylvania, Philadelphia, Pennsylvania 19104, United States

Supporting Information

ABSTRACT: Uranium compounds supported by redox-active α-diimine ligands, which have methyl groups on the ligand backbone and bulky mesityl substituents on the nitrogen atoms {$^{Mes}DAB^{Me}$ = [ArN═C(Me)C(Me)═NAr], where Ar = 2,4,6-trimethylphenyl (Mes)}, are reported. The addition of 2 equiv of $^{Mes}DAB^{Me}$, 3 equiv of KC_8, and 1 equiv of $UI_3(THF)_4$ produced the bis(ligand) species $(^{Mes}DAB^{Me})_2U(THF)$ (**1**). The metallocene derivative, $Cp_2U(^{Mes}DAB^{Me})$ (**2**), was generated by the addition of an equimolar ratio of $^{Mes}DAB^{Me}$ and KC_8 to Cp_3U. The bond lengths in the molecular structure of both species confirm that the α-diimine ligands have been doubly reduced to form ene-diamide ligands. Characterization by electronic absorption spectroscopy shows weak, sharp transitions in the near-IR region of the spectrum and, in combination with the crystallographic data, is consistent with the formulation that tetravalent uranium ions are present and supported by ene-diamide ligands. This interpretation was verified by U L_{III}-edge X-ray absorption near-edge structure (XANES) spectroscopy and by variable-temperature magnetic measurements. The magnetic data are consistent with singlet ground states at low temperature and variable-temperature dependencies that would be expected for uranium(IV) species. However, both complexes exhibit low magnetic moments at room temperature, with values of 1.91 and 1.79 μ_B for **1** and **2**, respectively. Iodomethane was used to test the reactivity of **1** and **2** for multielectron transfer. While **2** showed no reactivity with CH_3I, the addition of 2 equiv of iodomethane to **1** resulted in the formation of a uranium(IV) monoiodide species, $(^{Mes}DAB^{Me})(^{Mes}DAB^{Me2})UI$ {**3**; $^{Mes}DAB^{Me2}$ = [ArN═C(Me)C(Me$_2$)NAr]}, which was characterized by single-crystal X-ray diffraction and U M_4- and M_5-edge XANES. Confirmation of the structure was also attained by deuterium labeling studies, which showed that a methyl group was added to the ene-diamide ligand carbon backbone.

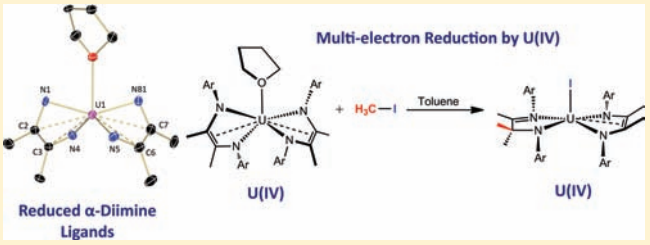

INTRODUCTION

Late transition metals readily participate in numerous chemical transformations currently exploited for use in industrial and pharmaceutical processes. Two-electron oxidative additions are often invoked as key steps in many of these reaction pathways. While this valuable reactivity is common for many d-block elements, it is not typically available to the f-block metals. Instead, for most lanthanides and actinides capable of redox chemistry, such as uranium, one-electron processes occur. As a result, oxidative addition chemistry analogous to that observed with late transition metals has only been observed sporadically with uranium.[1] Seminal studies have demonstrated the oxidative addition of alkyl halides by uranium(III) species through radical processes,[2−5] while more recent examples have shown that high-valent uranium(V) dimers are also capable.[6] In these examples, reducing equivalents must come from multiple uranium centers to accomplish two-electron oxidative addition, resulting in the addition of substrate to both uranium centers.

While multielectron processes have been observed for highly electron-rich uranium centers, such as cleavage of the N═N double bond in azobenzene to form uranium(VI) bis(imido) species,[7−9] this type of electron transfer chemistry is less common and difficult to access.[10−12] Recently, however, it has been shown that combining the reactivity of redox-active ligands with that of trivalent uranium facilitates the transfer of two or more electrons to a substrate.[13−15] For example, the dimeric uranium(III) complexes supported by $C_8H_8^{2-}$,[16−18]

Received: February 9, 2011
Published: July 15, 2011

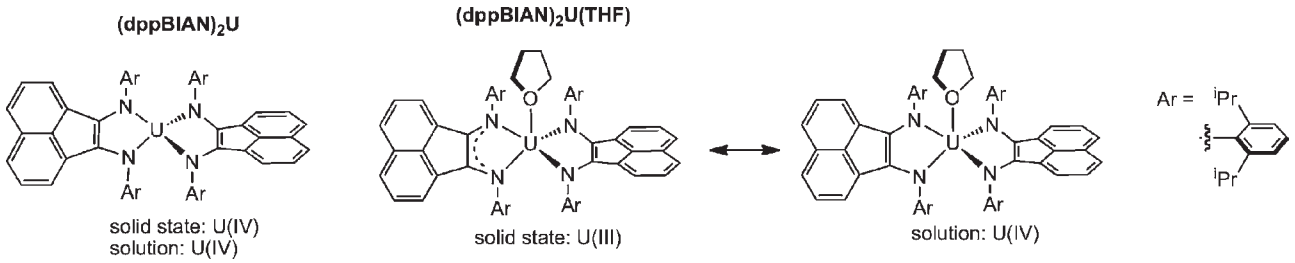

Figure 1. Uranium α-diimine complexes reported by Kiplinger et al.[29]

$MeC_6H_5^{2-}$,[19] $C_{10}H_8^{2-}$,[16] $C_6H_6^{2-}$,[18] and BPh_4^-,[20] and the monomeric species supported by 2,2′-bipyridine[21,22] all comprised of arene ligands that house one electron per uranium center. In combination with reducing equivalents from the uranium, these species have been shown to react as potent multielectron reductants toward small molecules.[19,20,22] In general, this reactivity relies on ligands that have energetically low-lying lowest unoccupied molecular orbitals (LUMOs), where electrons can be stored and transferred in discrete steps. The advantage of these frameworks is that they provide control for avoiding unwanted side reactions,[23] stabilize reactive species, and allow redox-inactive metals to engage in electron-transfer chemistry.[24] Recent advances have shown that redox-active ligands can control radical chemistry at readily available and inexpensive metals, transforming them into viable reagents for organometallic catalysis.[13,14,24−26]

While the use of redox-active ligands supporting trivalent uranium is documented in the literature,[19,20,27] using redox-active ligands with tetravalent uranium ions has only been recently explored. Gambarotta et al. have demonstrated the redox activity of the 1,3-bis(methylaryliminatobenzene) ligand through synthesis of a family of reduced uranium complexes.[28] In these studies, crystallography was paired with computation to show that electrons were stored in the π system of the ligand. Kiplinger et al. synthesized the first example of actinide compounds bearing α-diimine ligands by isolating uranium(III) and uranium(IV) compounds with reduced 1,2-bis[(2,6-diisopropylphenyl)imino]acenaphthylene (dppBIAN; Figure 1) ligands.[29] The bis(ligand) species, $(dppBIAN)_2U$, features a tetravalent uranium center with two dianionic ligands in both solution and the solid state, whereas the tetrahydrofuran (THF) analogue, $(dppBIAN)_2U(THF)$, was found to show variance in its oxidation state due to solvent coordination. This species has a trivalent uranium center, with one dianionic and one monoanionic ligand in the solid state but in solution behaves more like its base-free counterpart, with two dianionic dppBIAN ligands supporting a uranium(IV) center. These compounds proved to be highly reactive, and the preliminary studies showed that the compounds were only stable under very controlled conditions and readily decomposed to form complicated mixtures of products.

We set out to explore the reactivity of uranium complexes supported by the α-diimine ligand, $^{Mes}DAB^{Me}$, for multielectron-transfer chemistry ($^{Mes}DAB^{Me}$ = [ArN═C(Me)C(Me)═NAr], where Ar = 2,4,6-trimethylphenyl (Mes); note that the label $^{Mes}DAB^{Me}$ is used for both resonance structures of the ligand). Because this ligand has a simple C−C backbone rather than the conjugated framework associated with dppBIAN, we propose that these ligands can better maintain the accessibility of the stored electrons for oxidative addition given that the area for delocalization is much smaller. Additionally, we reasoned that $^{Mes}DAB^{Me}$ may provide additional stability from deleterious side reactions associated with dppBIAN. Herein we report the synthesis of $^{Mes}DAB^{Me}$ uranium(IV) species and their characterization by ^{1}H NMR and X-ray absorption spectroscopies, as well as X-ray crystallography and magnetometry. The reactivity of these species for multielectron activation of alkyl halides and full characterization of the subsequent products are also reported.

EXPERIMENTAL SECTION

General Considerations. All air- and moisture-sensitive manipulations were performed using standard Schlenk techniques or in an MBraun or Vacuum Atmospheres inert-atmosphere drybox with an atmosphere of purified nitrogen. The MBraun drybox was equipped with a cold well designed for freezing samples in liquid nitrogen as well as two −35 °C freezers for cooling samples and crystallizations. Solvents for sensitive manipulations were dried and deoxygenated using literature procedures with a Seca solvent purification system.[27] The toluene used for X-ray absorption near-edge structure (XANES) measurements was dried using sodium benzophenone, vacuum distilled, and degassed by three freeze−pump−thaw cycles. Benzene-d_6 was purchased from Cambridge Isotope Laboratories, dried with molecular sieves and sodium, and degassed by three freeze−pump−thaw cycles. Polystyrene (PolySciences Inc.) was acquired as 3.0 Micron Dry Form and dried under vacuum (10^{-3} Torr) for 24 h. Elemental analyses were performed by the microanalytical laboratory at the University of California—Berkeley, in Berkeley, CA, and Midwest Microlab, LLC, in Indianapolis, IN. NaCp (2.0 M in THF), naphthalene, and sodium were purchased from Sigma Aldrich and used as received. Methyl iodide and methyl-d_3 iodide were purchased from Sigma Aldrich, dried over $CaCl_2$, and vacuum transferred before use. $UI_3(THF)_4$,[30] potassium graphite,[31] D_{2d}-$CuCl_4Cs_2$,[32] $^{Mes}DAB^{Me}$,[33] and the UO_2[34] XANES standard (UO_3 and H_2 at 400 °C) were prepared according to literature procedures. The tetravalent $[NEt_4]_2[UCl_6]$ XANES energy standard was synthesized from a reaction between 2 equiv of $[NEt_4][Cl]$ and UCl_4 in THF, while the pentavalent $[NEt_4][UCl_6]$ standard was synthesized by refluxing $[NEt_4]_2[UO_2Cl_4]$ in thionyl chloride. Both molecular standards were characterized by single-crystal X-ray diffraction prior to analysis by XANES spectroscopy.

^{1}H NMR spectra were recorded on a Varian Inova 300 spectrometer operating at 299.992 MHz. All chemical shifts are reported relative to the peak for $SiMe_4$ using ^{1}H (residual) chemical shifts of the solvent as a secondary standard. For paramagnetic molecules, the ^{1}H NMR data are reported with the chemical shift, followed by the peak width at half-height in hertz, the integration value, and, where possible, the peak assignment. The spectra for paramagnetic molecules were obtained using an acquisition time of 0.5 s; thus, the peak widths reported have errors of ±2 Hz. Electronic absorption spectroscopic measurements were recorded at 294 K in THF in sealed 1 cm quartz cuvettes with a Jasco V-670 spectrophotometer. The mass spectrometry (MS) spectra

dx.doi.org/10.1021/ic2002805 |Inorg. Chem. 2011, 50, 9838–9848

were obtained on a Thermo Scientific LTQ Velos with an attached electrospray ionizer. The sample was diluted in acetonitrile and was infused at 5 μL/min with 3.5 kV ionization potential. MS/MS analysis was carried out in the linear ion trap with a variety of different collision energies.

XANES samples were prepared in a helium-filled glovebox, and the U L_{III}-edge ($^{Mes}DAB^{Me}$)$_2$U(THF) (**1**) and $Cp_2U(^{Mes}DAB^{Me})$ (**2**) samples were loaded into two nested aluminum sample holders equipped with Kapton windows. One set of windows was glued on, and one set was sealed with indium wire. The sample holder was shipped under helium in a sealed container that was opened at the beamline, immediately attached to the coldfinger of a liquid-N_2 cryostat, and quickly evacuated (10^{-5} Torr). The XANES measurements were conducted at the Stanford Synchrotron Radiation Lightsource (SSRL) under dedicated operating conditions (3.0 GeV, 5%, 100 mA) on end station 10-2. A single energy was selected from the white beam with a liquid-N_2-cooled double-crystal monochromator utilizing Si[220] crystals. The crystals were run fully tuned, and a flat platinum-coated mirror, tilted to have a cutoff energy of 20−22 keV, was used to eliminate harmonics. The room temperature (294 K) and low-temperature (77 K) measurements were calibrated to the energy of the first inflection point of a yttrium foil (17 032.08 eV), whose spectrum was measured within the same scan as the uranium analyte using the transmitted portion of the beam. The spectra were measured in the fluorescence mode using a Lidle detector and the transmission data measured using an ion chamber positioned after the sample. Dead times were set at ~1.2 μs. Using an in-house program, the averaged spectra were normalized to a per-atom basis by offsetting the spectrum so that the value of a polynomial fit through the preedge region equaled zero at 17 185 eV and then scaled so that the value of a polynomial fit through the postedge region equaled unity at this same energy. The exact position of the inflection point of the rising edge in each spectrum was determined by calculation of the first and second derivatives of the data.

The U M_5- and M_4-edge XANES samples were prepared by finely grinding the analyte (0.010 g) with polystyrene beads (0.120 g) to obtain a homogeneous mixture that contained, by mass, 8% analyte as described previously.[35] An aliquot of this mixture (0.020 g) was transferred to a vial that contained polystyrene (0.060 g), and this new diluted mixture was ground for 2 min to achieve small and finely divided particles. An aliquot of this mixture (0.060 g) was transferred to a vial, and toluene (0.400 mL) was added. The mixture was stirred with a glass rod until the polystyrene dissolved, and the mixture was transferred into a 5 × 11 × 4 mm well that had been bored into an aluminum block and fastened to a piece of Teflon backing. The toluene was allowed to evaporate for 48 h under the helium atmosphere of the glovebox, at which point the Teflon backing was removed, leaving a robust film fixed within the aluminum block. Spectra were collected in a chamber, similar to that previously described,[35,36] with the exception that the entire chamber was isolated from the beam pipe by a beryllium window and that the I_0 compartment was separated from the sample compartment by a 15 μm polypropylene film. The room temperature U M_5- and M_4-edge XANES spectra were recorded at SSRL using the 54-pole wiggler beamline 6-2 with a nickel-coated harmonic rejection mirror and a Si(111) double crystal monochromator that had been detuned by 50% (3150 eV). Data were collected under vacuum (10^{-6} Torr), and the sample excitation fluorescence was measured against the incident beam using pairs of backward-facing International Radiation Detector XUV100-type photodiodes coated with 1000 Å of aluminum. The photodiodes were closely spaced so that a 1−2-mm-wide beam passed between them, and the incident beam intensity was measured as the scatter off of the polypropylene window. The fluorescence from the sample was measured by an identically configured photodiode pair, which was mounted facing the sample at normal incidence to the oncoming beam. These detectors were sensitive to fluorescence over a wide solid angle because of their close proximity to the sample (5 mm). The energy calibrations for the Cl K-edge X-ray absorption spectroscopy (XAS) were repeatedly conducted between spectra and were based on the maximum of the first preedge feature in the Cl K-edge XAS of D_{2d}-Cs_2CuCl_4 at 2820.20 eV. For all XANES measurements, the exact position of the inflection point of the rising edge in each spectrum was determined by calculation of the first and second derivatives of the data.

Magnetic data were collected using a Quantum Design Magnetic Property Measurement System (MPMS-7) with a reciprocating sample option at 0.1 T from 2 to 300 K and at 2 K from 0 to 7 T. The MPMS-7 was calibrated to the nearest 10^{-3} emu using a palladium standard. Silylated, predried, and hardened gelatin capsules were used to hold the samples for measurement. The capsules were pretreated for 48 h with hexamethyldisilazane vapor followed by drying under a dynamic vacuum at 100 °C for 24 h. Analytically pure samples were massed to the nearest 0.1 mg in an inert-atmosphere (N_2) drybox using a calibrated and leveled Mettler-Toledo AL-204 analytical balance. The loaded capsules, enclosed in drinking straws for measurement, were transferred to the MPMS under an inert atmosphere and immediately loaded into the measurement chamber with three purge cycles. Corrections for the intrinsic diamagnetism of the compounds were made using Pascal's constants.[37] Measurements were made in duplicate on independently synthesized samples to verify the gross magnetic behavior of the compounds.

Single crystals for X-ray diffraction were coated with poly(isobutylene) oil in a glovebox and quickly transferred to the goniometer head of a Rigaku Rapid II image-plate diffractometer equipped with a MicroMax002+ high-intensity copper X-ray source with confocal optics. Preliminary examination and data collection were performed with Cu Kα radiation (λ = 1.541 84 Å). Cell constants for data collection were obtained from least-squares refinement. The space group was identified using the program *XPREP*.[38] The structures were solved using the structure solution program *PATTY* in *DIRDIFF99*.[39] Refinement was performed on a LINUX PC using *SHELX-97*.[38] The data were collected at a temperature of 150(1) K.

Synthesis of ($^{Mes}DAB^{Me}$)$_2$U(THF) (1). A 20 mL scintillation vial was charged with 0.317 g (0.350 mmol) of $UI_3(THF)_4$ and THF. During stirring, a THF solution of 0.224 g (0.700 mmol) $^{Mes}DAB^{Me}$ was added, immediately followed by 0.142 g (1.05 mmol) of KC_8. After stirring for 3 h, the solvent was removed from the dark-orange-brown solution in vacuo. Ether was added, and the solution was filtered over Celite to remove graphite and KI. The filtrate was concentrated and cooled to −35 °C to crystallize out any unreacted $^{Mes}DAB^{Me}$ ligand. The solution was decanted and dried under vacuum to afford ($^{Mes}DAB^{Me}$)$_2$U(THF) (**1**) as an orange-brown solid. The free ligand can be difficult to remove, lowering the yield. Thus, an alternative synthesis is presented.

Alternative Synthesis for ***1***. A 20 mL scintillation vial was charged with 0.020 g (0.883 mmol) of sodium and THF. During stirring, a catalytic amount of naphthalene (0.002 g, 3 mol %) and 0.142 g (0.442 mmol) of $^{Mes}DAB^{Me}$ was added, affording a red solution. This was stirred for 1 h or until all of the sodium was consumed. The red solution was added to 0.200 g (0.221 mmol) of $UI_3(THF)_4$ in THF (blue solution) and stirred for 3 h, followed by removal of the solvent in vacuo. The residue was taken up in an ether/pentane mixture and filtered over Celite, producing an orange-brown filtrate. The solvent was removed under vacuum to afford **1** as an orange-brown solid. Dark-orange crystals were obtained by recrystallization from pentane/ether (10:1) at −35 °C (0.199 g, 0.208 mmol, 94%). X-ray-quality single crystals were obtained under the same conditions. Elem anal. Calcd for $C_{48}H_{64}N_4OU$: C, 60.62; H, 6.70; N, 5.89. Found, C, 60.77; H, 6.51; N, 5.81. ^{1}H NMR (C_7D_8, 25 °C): δ −32.13 (281, 6H, CH_3), −15.39 (221, 6H, CH_3), −8.56 (378, 6H, CH_3), −3.10 (204, 8H, Ar*H* and CH_3), −1.67 (222, 8H, Ar*H* and CH_3), 8.45 (204, 6H, CH_3), 13.50 (18, 2H, Ar*H*), 22.83 (187, 2H, Ar*H*), 27.42 (258, 6H, CH_3), 68.91 (202, 6H, CH_3). ^{1}H NMR

dx.doi.org/10.1021/ic2002805 |*Inorg. Chem.* 2011, 50, 9838–9848

(C_7D_8, −40 °C): δ −85.07 (25.7, 2H, THF-CH_2), −58.56 (228, 2H, THF-CH_2), −37.98 (169, 6H, CH_3), −30.88 (279, 2H, THF-CH_2), −25.59 (262, 2H, THF-CH_2), −23.31 (242, 6H, CH_3), −14.21 (193, 6H, CH_3), −5.74 (124, 2H, Ar*H*), −5.19 (43, 6H, CH_3), −3.11 (19, 6H, CH_3), −2.73 (44, 2H, Ar*H*), 10.52 (26, 6H, CH_3), 15.74 (34, 2H, Ar*H*), 27.51 (89, 2H, Ar*H*), 33.75 (185, 6H, CH_3), 88.40 (605, 6H, CH_3). ^{1}H NMR (C_7D_8, −60 °C): δ −93.52 (634, 2H, THF-CH_2), −63.63 (481, 2H, THF-CH_2), −40.47 (247, 6H, CH_3), −33.98 (276, 2H, THF-CH_2), −26.94 (489, 8H, THF-CH_2 and CH_3), −16.87 (285, 6H, CH_3), −7.46 (164, 2H, Ar*H*), −6.13 (74, 6H, CH_3), −3.81 (51, 8H, Ar*H* and CH_3), 11.45 (39, 6H, CH_3), 16.94 (49, 2H, Ar*H*), 29.62 (182, 2H, Ar*H*), 36.72 (300, 6H, CH_3), 97.00 (848, 6H, CH_3).

Synthesis of $Cp_2U(^{Mes}DAB^{Me})$ (2). A 20 mL scintillation vial was charged with 0.261 g (0.288 mmol) of $UI_3(THF)_4$ and THF. During stirring, 0.089 g (1.01 mmol) of sodium cyclopentadienide (NaCp; 2 M in THF) was added. An excess of this reagent was added to ensure that all of the $UI_3(THF)_4$ reacted to produce Cp_3U in situ. (Note: Cp_3U can also be filtered at this point and isolated for future reaction.) If the excess is not used, compounds **1** and **2** are made simultaneously. After 3 h, the solution changed from blue to green with a white precipitate, and 0.092 g (0.288 mmol) of $^{Mes}DAB^{Me}$ and 0.117 g (1.75 mmol) of KC_8 were successively added during stirring. After 3 h more, the solution color changed from green to dark red-brown and was filtered over Celite to remove KCp, NaI, and graphite. The volatiles were removed in vacuo. The resulting solid was dissolved in a minimal amount of ether, transferred to a scintillation vial, and cooled to −35 °C to crystallize out any unreacted $^{Mes}DAB^{Me}$ ligand. The mother liquor was decanted, transferred to a vial, and dried under vacuum, affording $Cp_2U(^{Mes}DAB^{Me})$ (**2**) as a brown-red solid. As is the case with **1**, the free ligand can be difficult to remove, lowering the yield. Thus, an alternative synthesis is presented.

Alternative Synthesis for ***2***. As described above, Cp_3U was generated. In parallel, a 20 mL scintillation vial was charged with 0.013 g (0.546 mmol) of sodium and THF. During stirring, a catalytic amount 0.002 g (3 mol %) of naphthalene and 0.860 g (0.442 mmol) of $^{Mes}DAB^{Me}$ were added, affording a red solution. This was stirred for 1 h or until all of the sodium was consumed. This red solution was added to the previously prepared green solution of Cp_3U at room temperature. After 3 h, the solution color changed from green to dark brown-red and the volatiles were removed in vacuo. The residue was taken up in ether/pentane and filtered over Celite to remove NaI and NaCp, yielding a brown-red filtrate, which was dried under vacuum, affording **2** as a brown-red solid. Dark-red crystals were obtained by recrystallization from pentane/ether (10:1) at −35 °C (0.277 g, 0.402 mmol, 91%). X-ray-quality single crystals were obtained under the same conditions. Elem anal. Calcd for $C_{32}H_{38}N_2U$: C, 55.81; H, 5.56; N, 4.07. Found, C, 55.59; H, 5.55; N, 3.97. ^{1}H NMR (C_6D_6, 25 °C): δ −40.73 (4, 6H, CH_3), −19.87 (5, 6H, CH_3), −7.02 (3, 6H, CH_3), −0.35 (5, 2H, Ar*H*), 2.62 (2, 5H, Cp*H*), 12.53 (5, 5H, Cp*H*), 12.83 (5, 2H, Ar*H*), 24.53 (4, 6H, CH_3).

Synthesis of $(^{Mes}DAB^{Me})(^{Mes}DAB^{Me2})UI$ (3). A 20 mL scintillation vial was charged with 0.146 g (0.153 mmol) of **1**, a stir bar, and toluene. While stirring, 19 μL (0.305 mmol) of iodomethane was added. Upon addition, the orange suspension dissolved to form a brown solution that was subsequently stirred for 1 h. A white solid precipitated during the course of the reaction, and was removed by filtering the reaction mixture through Celite. The filtrate was dried in vacuo to yield **3** as a brown solid (0.132 g, 0.129 mmol, approximately 80%). Because of the difficulty in removing the white solid, a reliable combustion analysis could not be obtained. ^{1}H NMR (C_6D_6, 25 °C): δ −45.71 (14, 6H, CH_3), −15.79 (36, 3H, CH_3), −12.22 (6, 3H, CH_3), −11.63 (12, 3H, CH_3), −5.94 (4, 3H, CH_3), −2.14 (3, 6H, CH_3), 2.87 (3, 12H, *p*-CH_3 on $^{Mes}DAB^{Me}$), 4.83 (36, 3H, CH_3 derived from CH_3I/CD_3I, determined by deuterium labeling), 6.70 (6, 2H, Ar*H* on $^{Mes}DAB^{Me2}$), 7.20 (4, 2H, Ar*H* on $^{Mes}DAB^{Me2}$), 7.84 (3, 6H, CH_3), 16.95 (6, 3H, CH_3), 46.63 (21, 4H, Ar*H* on $^{Mes}DAB^{Me}$), 53.04 (27, 3H, CH_3).

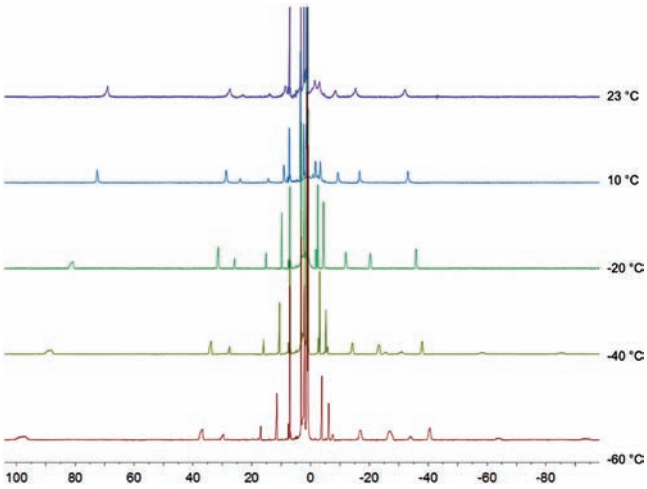

Figure 2. Variable-temperature ^{1}H NMR spectra for **1** in toluene-d_8.

RESULTS AND DISCUSSION

Synthesis of Uranium Derivatives. Initial experiments were aimed at metalation of the α-diimine ligand, $^{Mes}DAB^{Me}$, followed by reduction of the new uranium species to access the redox-active nature of the ligands. A total of 2 equiv of $^{Mes}DAB^{Me}$ was stirred with 1 equiv of $UI_3(THF)_4$ for 16 h in THF. After removal of the solvent, analysis by ^{1}H NMR spectroscopy confirmed that no reaction had occurred, likely because the soft nitrogen donor ligands are not suitable for such an electron-rich uranium center. Because the neutral ligands would not create an isolable species, metalation and reduction chemistry were attempted in a single step. The addition of 2 equiv of $^{Mes}DAB^{Me}$ and 3 equiv of KC_8 to $UI_3(THF)_4$ resulted in an orange-brown solution after 3 h. Following filtration and crystallization, the solid obtained was assigned as **1** (eq 1) because very little free $^{Mes}DAB^{Me}$ was recovered.

Analysis by ^{1}H NMR spectroscopy (benzene-d_6) revealed a paramagnetically shifted and highly broadened spectrum with 10 peaks ranging from −33 to +70 ppm, which is surprising given that f^2 uranium complexes generally display narrower lines than those observed for **1**. At ambient temperature, the spectrum shows eight resonances, consistent with inequivalent methyl groups throughout the ene-diamide ligand. Further, these peaks have integration values for six protons, indicating that the ligands are in a C_2 arrangement in solution. The spectrum also shows two resonances at 13.50 and 22.83 ppm that integrate to 2H, assignable to the aryl groups of the ligand. The final two resonances for these aryl groups expected at this temperature are not visible because of overlap of two of the broad methyl resonances. Those resonances for the THF ligand are broadened into the baseline and are not visible at this temperature.

The extreme broadness of the spectrum of **1** is most likely due to the dynamics of the compound in solution. To further elucidate the ^{1}H NMR spectrum of **1**, variable-temperature data were collected from room temperature to −70 °C in 10 °C increments (toluene-d_8), and selected spectra are presented in Figure 2 (a full chemical shift table and all variable-temperature spectra are presented in the Supporting Information, Table S1 and Figures S1−S3). Upon cooling to 10 °C, the methyl resonances begin to sharpen, making the two additional aryl resonances visible between 0 and −4 ppm. They are practically

dx.doi.org/10.1021/ic2002805 |*Inorg. Chem.* 2011, 50, 9838–9848

baseline-resolved at 0 °C, and at −10 °C they begin to shift upfield. At −20 °C, the aryl resonance on the right (−3.76 ppm at −10 °C) is completely obscured by the adjacent methyl peak at −4.44 ppm and, upon reaching −40 °C, now appears on the other side of the methyl peak. At −60 °C, the aryl resonance between 0 and −2 ppm displays similar behavior and is now completely obscured by its adjacent methyl peak, remaining there even at −70 °C.

Cooling the samples also makes the resonances for the THF ligands visible. At −30 °C, the broad resonances for the coordinated THF peaks begin to appear in the baseline. Four distinct peaks are observed at −40 °C at −25.59, −30.88, −58.56, and −85.07 ppm and become larger in intensity as the sample is cooled. At −60 °C, the resonance at −25 ppm shifts slightly to −26.94 ppm and is fully obscured by a methyl peak moving in an upfield direction. The other THF resonances between −60 and −80 ppm shift upfield during the change to low temperature.

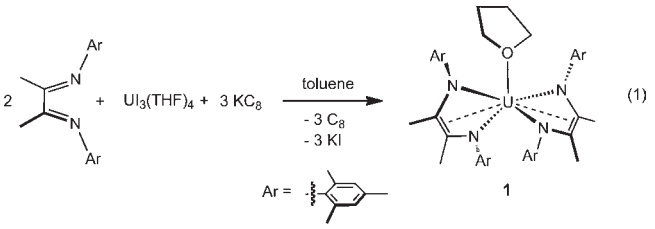

The synthesis of a uranium complex with cyclopentadienyl ligands was attempted to determine the extent of reduction of a 1:1 uranium-ene-diamide complex. Unsubstituted cyclopentadienyl ligands were used as supporting ligands and were metalated via salt metathesis. The addition of 3.5 equiv of NaCp to a stirring solution of $UI_3(THF)_4$ in THF resulted in a white precipitate (NaI) and a green solution assigned as Cp_3U. An excess of NaCp was necessary to ensure that all of $UI_3(THF)_4$ was consumed, preventing the formation of **1** during subsequent reduction. After workup, a single resonance was visible by ^{1}H NMR spectroscopy, supporting the formation of Cp_3U. To this THF solution was added 1 equiv of ^{Mes}DAB^{Me}, followed by 1 equiv of KC_8. Filtering, isolation, and recrystallization produced a brown-red solid assigned as **2** (eq 2).

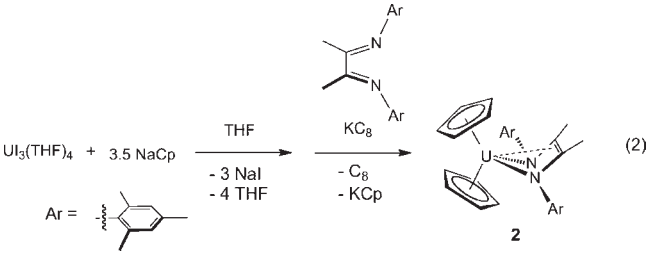

The ^{1}H NMR spectrum of **2** recorded in benzene-d_6 at ambient temperature greatly contrasts that of **1**. The spectrum shows peaks over a smaller range, −40.73 to +24.53 ppm (see the Supporting Information, Figure S4). Comparatively, the resonances are much sharper and have the appropriate number and integration for a C_s-symmetric molecule that is static at room temperature on the NMR time scale. The two resonances for the inequivalent cyclopentadienyl ring hydrogen atoms each integrate to five protons and appear at 2.62 and 12.53 ppm. Two peaks are observed for the inequivalent protons on the aryl groups appearing at −0.35 and +12.83 ppm. The rest of the methyl peaks on the mesityl rings and the ligand backbone each integrate to six protons and are indistinguishable based on these values. Heating of this sample to 50 °C in the NMR probe did not result in coalescence of the resonances but led to decomposition, as evidenced by the formation of a free ligand.

X-ray Crystallography. Aryl-substituted α-diimine ligands have been thoroughly studied on transition metals and lanthanides.[40−42] Population of their energetically low-lying π^* LUMOs (Figure 3a) has been established to cause structural distortions along the NCCN frame in accordance with the respective antibonding and bonding interactions depicted.[43] Compared to the neutral α-diimine ligand, the reduced version displays elongation of the C−N imine bonds and a contraction of the adjacent C−C bond by X-ray crystallography. Uncomplexed, neutral α-diimine ligands that have methyl substituents on the carbon atoms and substituted aryl groups typically have C═N double-bond distances ranging from 1.27 to 1.28 Å and C−C single-bond distances ranging from 1.49 to 1.51 Å.[44−47] The transfer of one electron from the metal center to the ligand results in moderate distortions, creating C−N bond distances of 1.32−1.35 Å with variable C−C distances. More extreme distortions occur from two-electron reduction where C−N distances of 1.40−1.42 Å and C−C distances of 1.35−1.40 Å are typically observed,[44−47] generating the ene-diamide resonance form of the ligand (Figure 3b). Another useful diagnostic feature for these species is the metal−nitrogen bond distance, which shortens as this interaction changes from a dative bond to an anionic bond.

Compound **1** was characterized by X-ray crystallography to determine the molecular structure and degree of reduction occurring in the ligand. Orange crystals suitable for X-ray diffraction were grown by cooling a concentrated THF solution of **1** to −35 °C. Analysis confirmed the identity of **1** as $(^{Mes}DAB^{Me})_2U(THF)$ (Figure 4), as was predicted based on the stoichiometry of the reaction. Compound **1** consists of a five-coordinate uranium center with a distorted square-pyramidal geometry. The THF molecule in the apical position of the pyramid is disordered.

The structural parameters for **1** (Table 1) reveal that a complete reduction of the α-diimine ligands has occurred; the magnitude of the structural distortions in the ligands is consistent with the formation of ene-diamide ligands, indicating that **1** contains a tetravalent uranium center. The N−C distances of 1.431(7), 1.419(6), 1.432(6), and 1.418(6) Å are increased significantly compared to those in the free ^{Mes}DAB^{Me} ligand of 1.278(2) Å, whereas the C−C distances of 1.361(8) and 1.364(7) Å have contracted greatly [compared to 1.500(2) Å in free ^{Mes}DAB^{Me}].[44] These distortions confirm population of the π^* orbitals and support two-electron reduction because they are even more extreme than those observed by Kiplinger et al. for the trivalent $(dpp\text{-}BIAN)_2U(THF)$, which has both dianionic and monoanionic ligands. Despite coordination of THF, the more appropriate comparison is with the solvent-free uranium(IV) complex, $(dpp\text{-}BIAN)_2U$, which is established to have two doubly reduced chelators. This complex exhibits N−C distances ranging from 1.378(11) to 1.415(11) Å and C−C distances of 1.410(12) and 1.412(12) Å. Thus, the strong deviation of the distances in **1** from the free ligand values supports the formulation of **1** as a uranium(IV) species with two dianionic ligands.

In addition to distortions within the ligand, the U−N bond distances are also indicative of ligand reduction. The dative U−N

dx.doi.org/10.1021/ic2002805 |Inorg. Chem. 2011, 50, 9838–9848

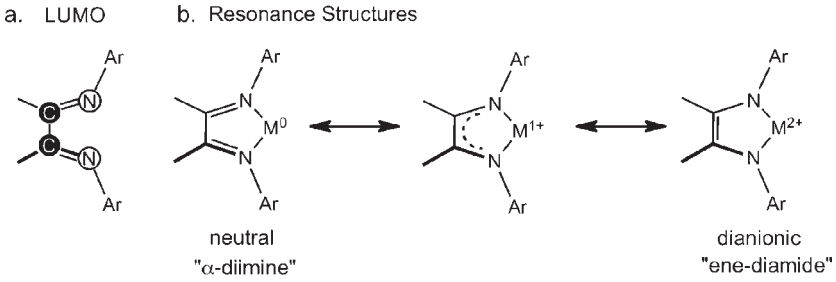

Figure 3. Top view of *p*-orbitals of LUMO for the α-diimine ligand (a) and resonance structures for α-diimine (b) bound to a metal in various oxidation states.

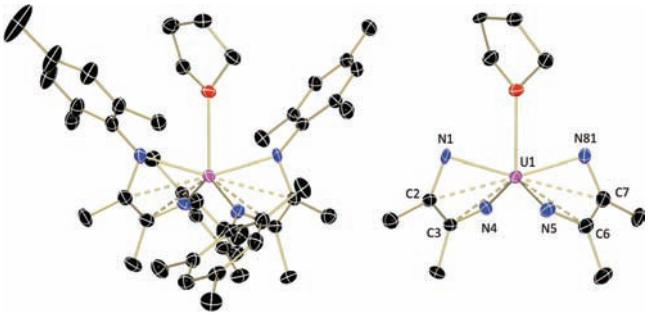

Figure 4. Molecular structure of **1** shown with 30% probability ellipsoids. Hydrogen atoms and solvent molecules have been omitted for clarity. The structure on the right shows the core of the molecule with the aryl groups removed.

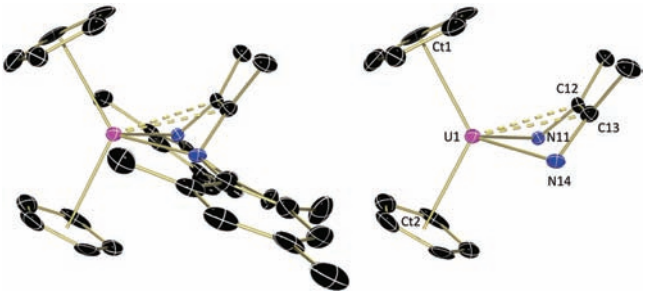

Figure 5. Molecular structure of **2** shown with 30% probability ellipsoids. Hydrogen atoms and solvent molecules have been omitted for clarity. The structure on the right shows the core of the molecule with the aryl groups removed.

Table 1. Bond Distances for Free $^{Mes}DAB^{Me}$ for 1−3

compound	C−N	C−C	U−N	U−$C_{diimine}$	U−C_{Cp}
$^{Mes}DAB^{Me}$ [44]	1.278(2)	1.500(2)			
1	1.431(7)		2.251(4)	2.749(5)	
	1.419(6)	1.361(8)	2.252(4)	2.773(4)	
	1.432(6)	1.364(7)	2.255(3)	2.787(6)	
	1.418(6)		2.255(4)	2.788(5)	
2				2.637(7)	2.701(9), 2.715(8)
				2.685(5)	2.720(9), 2.735(9)
	1.425(10)	1.399(1)	2.224(6)		2.735(8), 2.759(8)
	1.407(9)		2.198(6)		2.764(8), 2.772(9)
					2.788(9), 2.792(9)
3	1.30(2)		2.492(11)	2.708(15)	
	1.42(2)	1.49(2)	2.320(14)	2.710(18)	
	1.41(2)	1.37(2)	2.197(13)		
	1.37(2)		2.272(15)		

interaction associated with diimine groups has a long bond, which shortens considerably when an anionic bond between the nitrogen atoms and the uranium is made in the ene-diamide resonance form. The U−N bond distances in **1** of 2.251(4), 2.253(4), 2.255(3), and 2.255(4) Å are comparable to those reported for $(dpp\text{-}BIAN)_2U$ [ranging from 2.242(7) to 2.283(7) Å]. In addition, both compounds have U−N distances similar to those reported in uranium(IV) amide complexes, supporting the formulation of these ligands as dianionic.[48]

As shown in the resonance structure for the ene-diamide ligand (Figure 3), extreme reduction of the α-diimine ligand results in the formation of a double bond between the two carbon atoms of the ligand backbone. The molecular structure of **1** shows that the ligands are, in fact, not flat with respect to the uranium ene-diamide plane but bent toward the uranium ion, resulting in an interaction of the C−C π bond with the uranium ion. The observed U−C distances of 2.749(5), 2.773(4), 2.787(6), and 2.788(5) Å are on the order of those observed previously for uranium interactions with C−C π bonds.[49]

Red hexagonal crystals of **2** were grown by cooling a concentrated THF solution to −35 °C. Analysis confirmed the identity of **2** as $Cp_2U(^{Mes}DAB^{Me})$ (Figure 5), with a four-coordinate uranium center with pseudotetrahedral geometry. Structural parameters for **2** (Table 1) indicate that $^{Mes}DAB^{Me}$ has again been reduced, with C−N bonds elongated to 1.425(10) and 1.407(9) Å and a C═C distance contracted to 1.399(1) Å from the bonds in free $^{Mes}DAB^{Me}$.[44] As anticipated, the U−N bond distances are shorter in **2** [2.224(6) and 2.198(6) Å] than in **1** and are attributed to the reduced steric crowding about the metal center, allowing for a tighter ligand coordination. Nonetheless, the metrical parameters of **2** support two-electron reduction of the α-diimine ligand, indicating a tetravalent uranium center.

Similar to **1**, compound **2** features an association of the C═C bond of the ligand backbone to the uranium, causing the back of the ligand to rise from the U−N−N plane (dotted bonds in Figure 5). This results from the sterically accessible uranium center, a direct result of the unsubstituted cyclopentadienyl ligands in **2** compared to the additional ene-diamide and THF ligands in **1**. The U−C bond distances of 2.673(7) and 2.685(8) Å are shorter than those observed from the uranium to the cyclopentadienyl rings, indicating that this is a potentially important bonding interaction in these complexes. These distances are similar to those previously observed by Cloke for the uranium deltate dimer, $[U_2(\eta^8\text{-}COT^{\dagger})_2(\eta^5\text{-}Cp^*)]_2(\mu\text{-}\eta^1\text{:}\eta^2\text{-}C_3O_3)$ [$COT^{\dagger}$ = 1,4-bis(triisopropylsilyl)cyclooctatetraenide; Cp^* = 1,2,3,4,5-pentamethylcyclopentadienide], which has U−C distances of 2.654(4) and 2.670(4) Å.[50]

dx.doi.org/10.1021/ic2002805 |*Inorg. Chem.* 2011, 50, 9838–9848

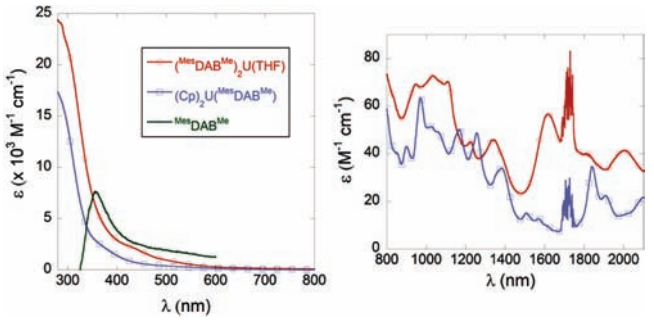

Figure 6. Electronic absorbance spectra of free $^{Mes}DAB^{Me}$ (green), **1** (red), and **2** (blue) recorded in THF. The UV−vis region is presented on the left and the near-IR region on the right. Note: Sharp peaks at ∼1650−1750 nm in both spectra are due to the second harmonic of the THF solvent.

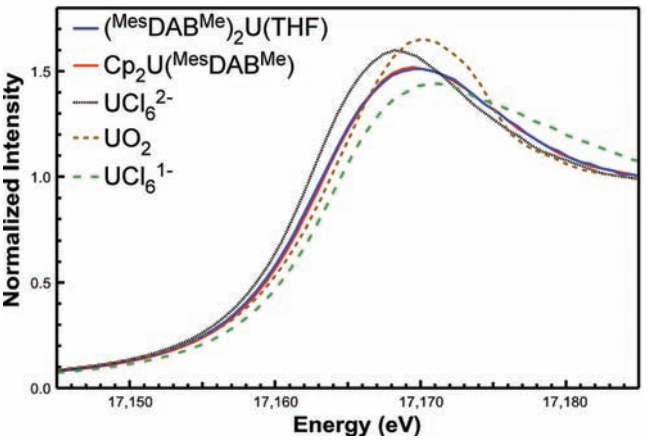

Figure 7. U L_{III}-edge XANES data for **1** (blue, solid) and **2** (red, solid) overlaid on some representative XANES standards, namely, $[NEt_4]_2[UCl_6]$ (gray, dotted), UO_2 (brown, dashed), and $[NEt_4][UCl_6]$ (green, dashed).

Although derivatives **1** and **2** were synthesized using uranium(III) starting materials and potassium graphite, oxidation of the uranium center occurs under these reducing conditions to generate uranium(IV) products. While this transformation is complicated, it seems highly likely that the uranium(III) ion plays a part in the reduction of the $^{Mes}DAB^{Me}$ ligands, thus taking advantage of the redox-active nature of α-diimines. Attempts at synthesizing the THF free analogue of **1** in analogy to $(dppBIAN)_2U$ either by use of UCl_4 and reducing agents or by thermolysis of **1** under vacuum have been unsuccessful, indicating that THF plays an important role in stabilization.

Electronic Absorption Spectroscopy. Characterization by electronic absorption spectroscopy was performed to examine the formulation of **1** and **2** as uranium(IV) species. Spectra for **1** (blue), **2** (red) and free $^{Mes}DAB^{Me}$ (green) were collected from 300 to 2200 nm in THF at ambient temperature (Figure 6). For uncoordinated $^{Mes}DAB^{Me}$, there is an intense absorption at 300 nm, which is assignable to a ligand-based $\pi-\pi^*$ transition. The uranium species exhibit a peak at λ_{max} = 355 nm, with ε values of 3640 M^{-1} cm^{-1} (**1**) and 9240 M^{-1} cm^{-1} (**2**), and are assigned as ligand-to-metal charge-transfer bands. At lower energy in the near-IR region, a series of sharp bands with weak intensity can be observed for **1** and **2**; the band positions and intensities are characteristic of f^2 uranium(IV) compounds.[51,52] These are assigned as f−f transitions because their energy and molar absorptivities, which range from about 10 to 140 M^{-1} cm^{-1}, are consistent with those observed previously for tetravalent uranium in $(dpp\text{-}BIAN)_2U(THF)$.[29]

X-ray Absorption Spectroscopy. In order to evaluate the effective nuclear charge on the uranium ions in **1** and **2**, U L_{III}-edge XANES experiments were carried out on samples at room temperature and 77 K (Figure 7). All spectra were calibrated in energy to the first inflection point of an yttrium foil (17 032.08 eV), whose spectrum was measured within the same scan as the uranium analyte using the transmitted portion of the beam. For both compounds, the XANES spectra collected at 294 K are nearly identical with the spectra obtained at 77 K. The first and second derivative analyses show that both data sets contain a single postedge peak at 17 169 eV, and the inflection points for the rising edges in both spectra occur at 17 163 eV. In Figure 7, these data are compared with the U L_{III}-edge XANES spectra collected on some representative standards, namely, UO_2, $[NEt_4]_2[UCl_6]$, and $[NEt_4][UCl_6]$. This shows that the rising edges for compounds **1** and **2** are significantly lower in energy than that observed for the pentavalent $[UCl_6]^-$ compound and bracketed by the rising edges for the tetravalent UO_2 and $[UCl_6]^{2-}$ species. Overall this analysis suggests that compounds **1** and **2** are supported by dianionic $^{Mes}DAB^{Me}$ ligands and contain uranium ions with two 5f electrons.

Magnetism. Temperature- and field-dependent magnetic data were collected for **1** and **2** in the range of 2−300 K at 0.1 T and from 1 to 7 T at 2 K (Figure 8). The data for the two compounds are similar and show moments of 0.68 and 0.40 μ_B at 2 K for **1** and **2**, respectively, calculated at those temperatures from their χT products. The negligible moments at 2 K and the field-dependent data (Figure 8, insets) indicate singlet ground states for both complexes, which is typical for molecular uranium(IV) complexes with low site symmetry at the metal ion.[53−55] The temperature dependencies for **1** and **2** also support this oxidation-state assignment. The χT products decrease gradually with the temperature until ∼100−150 K, where the onset of the singlet ground state begins to dominate the data with depopulation of crystal-field excited states. Reported room temperature magnetic moments of $5f^2$ uranium(IV) compounds with tetragonal or lower symmetry rarely achieve the Curie value of 3.58 μ_B because of crystal-field splitting of the $^3H_4$ ground term. In this case, the room temperature magnetic moments of **1** and **2** are 1.91 and 1.79 μ_B, respectively. These values are quite low considering that empirical room temperature magnetic moments for previously reported uranium(IV) complexes range from ∼2.5 to 3.1 μ_B.[10,29,56−58]

The origin of the unusually low room temperature magnetic moments of **1** and **2** is unclear. The related $U(dpp\text{-}BIAN)_2$ has a room temperature magnetic moment of 2.77 μ_B, which is larger than that of **1** and typical for molecular uranium(IV) complexes.[29] Reported pentamethylcyclopentadienyluranium(IV) bis(ketimide) complexes provide a useful comparison for **2**.[53] Both **2** and the reported bis(ketimides) have C_{2v} site symmetries and roughly similar ligand fields comprising anionic nitrogen donors. The uranium(IV) bis(ketimides) show room temperature moments of ∼2.7 μ_B, which is also typical for molecular uranium(IV) compounds and larger than the moment found for **2**.[53] Considering the small room temperature moments of **1** and **2**, covalent uranium−ligand bonding has been suggested in the literature as one factor in attenuating the moments of such

dx.doi.org/10.1021/ic2002805 |Inorg. Chem. 2011, 50, 9838–9848

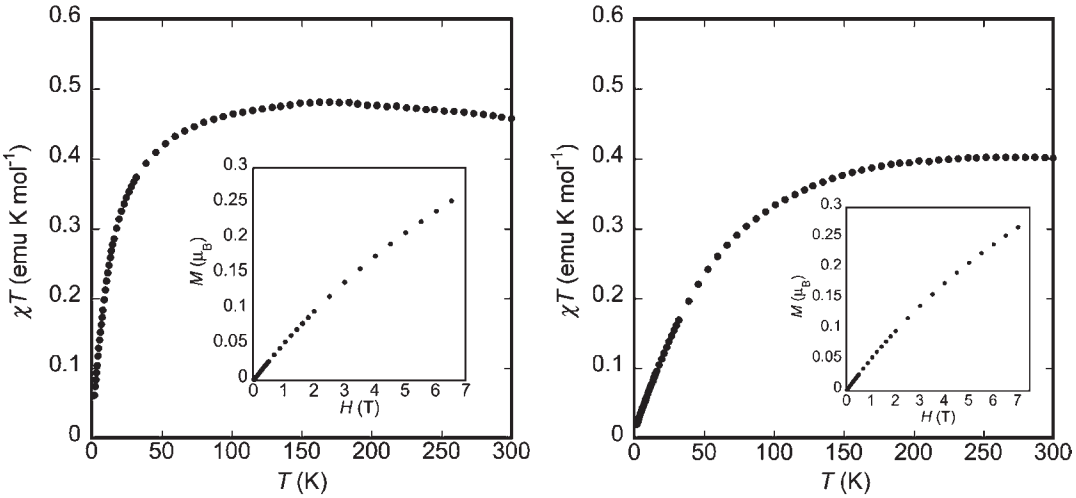

Figure 8. Temperature- and field-dependent (insets) magnetic data for **1** (left) and **2** (right). Temperature-dependent data were collected at 0.1 T, and field-dependent data were collected at 2 K.

complexes.[59,12] However, in cases where 5f-orbital covalency is specifically implicated, the characteristic temperature-dependent behavior of low-symmetry uranium is altered.[60] Because of the normal temperature dependencies displayed by **1** and **2**, uranium−ligand covalency is not expected to play a primary role in determining their room temperature moments, as is supported by the XANES data for these complexes. Further, **1** and **2** are stable in air in the solid state, attesting to the fact that decomposition is not suspected to be responsible for the unusual magnetic data.

Because both **1** and **2** consistently show the lower than expected moments in duplicate measurements on unique samples, we postulate that their low moments are the result of a common electronic phenomenon arising from interaction of the redox-active ene-diamide ligand with the uranium ions.[61] A positive correlation between the uranium−ene bond distances and the room temperature magnetic moments of **1** and **2** is noted. Although the magnetic data are unusual, the physicochemical data for **1** and **2** support an assignment of the uranium ions as tetravalent with two redox non-innocent dianionic ene-diamide ligands. It must be cautioned that detailed analysis of the magnetic data is, at present, underparametrized with respect to ligand-field splittings, electronic state mixing, and the potential for redox noninnocence. Further studies are underway to expand the correlation of the uranium−ene bond distances and the room temperature magnetic moments of the complexes. Additional work is ongoing using the tools of theory to elucidate noninnocence contributions to the uranium−ligand bonding in **1** and **2** toward a comprehensive model of the electronic structures of the complexes.

Reactivity toward Iodomethane. Compounds **1** and **2** were explored to determine the role, if any, of the redox-active α-diimine ligands in subsequent reactivity. Specifically, multielectron activation of alkyl halides to the uranium center was targeted to determine if the electrons localized on the ligand are a source of reducing equivalents for subsequent chemistry. Because of the extremely bulky mesityl groups on the supporting ligands, the smallest alkyl halide, iodomethane CH_3I, was explored. The addition of 1 equiv of iodomethane to **1** resulted in the formation of a new product in 50% conversion, as judged by ^{1}H NMR spectroscopy. Exposing **1** to a second equiv of CH_3I resulted in complete conversion to a brown uranium-containing product (**3**) and the formation of a white solid, which was separated from **3** by vacuum filtration (eq 3). Characterization of the brown complex, **3**, by ^{1}H NMR spectroscopy revealed a paramagnetically broadened and shifted spectrum consistent with a C_1-symmetric uranium species exhibiting 14 resonances distributed between −46 and +54 ppm (see the Supporting Information, Figure S4). The use of iodomethane-d_3 produced the isotopomer of **3** (**3**-d_3), which shows a broad methyl resonance at 4.83 ppm by ^{2}H NMR spectroscopy; the absence of the corresponding methyl resonance was observed in the ^{1}H NMR spectrum of **3**-d_3.

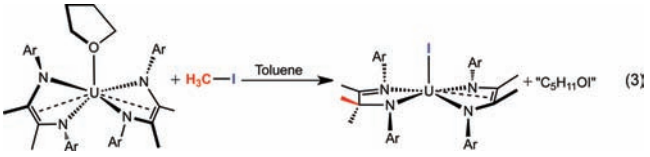

Interestingly, the product from the reaction with iodomethane, **3**, does not retain the THF ligand present in the starting material **1**. Over the course of this reaction, however, a white precipitate is observed in the reaction and is proposed to be the product of the THF ligand reacting with 1 equiv of iodomethane. Although difficult to firmly identify by ^{1}H NMR spectroscopy because it is generated in small quantities, mass spectrometry confirmed the formula of the organic compound as $C_5H_{11}OI$, formed by the reaction of CH_3I with coordinated THF.

Single crystals of **3** grown from a concentrated pentane solution cooled to −35 °C were further characterized by X-ray diffraction. The molecular structure of **3** revealed (^{Mes}DAB^{Me})-(^{Mes}DAB^{Me2})UI {^{Mes}DAB^{Me2} = [ArN═C(Me)C(Me)$_2$-NAr]}, the product of iodomethane addition to **1** (Figure 9). Complex **3** features a five-coordinate uranium center in a distorted square-pyramidal geometry, with an iodide ligand coordinated to the uranium ion and a methyl group appended to one of the two diimine ligand backbones to form a localized monoanionic ligand with an imine substituent. Because of the presence of the new methyl group, the double-bond character in the C12−C13

dx.doi.org/10.1021/ic2002805 |*Inorg. Chem.* 2011, 50, 9838–9848

α-diimine backbone is lost, and direct U−C bonding interactions are not observed for the $^{Mes}DAB^{Me2}$ ligand.

The metrical parameters for **3** are presented in Table 1. The large uncertainties associated with the data set for **3** preclude a detailed discussion of the bond distances within the ligand framework. The U−N distances, however, are precisely determined and are reliable reporters on the extent of ligand reduction. The U−N distances for N21 and N24 of 2.197(13) and 2.272(15) Å, respectively, are in accordance with those observed for complexes **1** and **2** [2.198(6)−2.255(4) Å], consistent with a doubly reduced α-diimine ligand. The U−N bond distances in the imine−amide supporting ligand differ as expected based on the presence of the additional methyl group located at C13. The presence of the methyl group creates an sp^3-hybridized carbon, forcing a single bond between C13 and N14 [1.42(2) Å] and an anionic bond between U1 and N14. The latter distance is 2.320(14) Å and slightly longer than that observed for the U−N distance for the reduced ligand in the starting complex **1**. Another result from the addition of the methyl group at the C13 position is the restoration of a double bond between C12 and N11 [1.30(2) Å], which creates a dative U1−N11 interaction. The long bond length of 2.492(11) Å confirms this because it is significantly longer (greater than 3σ) than the anionic U−N distances in the starting complex. Although less significant, the C12−C13 distance [1.49(2) Å] for this ligand is much longer than those in **1** and the reduced ligand in **3**, further indicating the loss of an electron in this ligand.[44] Overall, the U−N distances in **3** support the theory that one ligand is dianionic and the other is monoanionic with a dative interaction. Coupling these observations to the presence of the iodine ligand, an oxidation state of uranium(IV) can be formulated for the uranium center in **3**. The observed reaction of **1** with iodomethane is in sharp contrast to that previously reported with cyclopentadienyluranium(III) species[2−5] because the ene-diamide derivatives do not require 2 equiv of uranium for C−I bond cleavage.

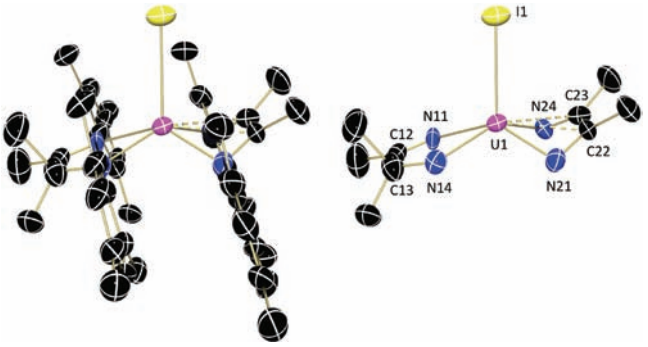

Figure 9. Molecular structure of **3** shown with 30% probability thermal ellipsoids. Hydrogen atoms and solvent molecules are omitted for clarity. The structure on the right shows the core of the molecule with the aryl groups removed.

Understanding the molecular structure of **3** allows a more detailed discussion of the observed ^1H NMR spectrum (benzene-d_6, with the labeling scheme and spectrum presented in the Supporting Information, Figure S5). There are 14 paramagnetically broadened and shifted resonances that appear with the following integration values (no. of resonances in parentheses): 12 (1) : 6 (3) : 4 (1) : 3 (7) : 2 (2). The inequivalency in the spectrum is due to the presence of two different ligands, $^{Mes}DAB^{Me}$ and $^{Mes}DAB^{Me2}$, coordinated to the uranium center. In addition, the number and integration values of the resonances for the aryl rings indicate that they are not rotating on the NMR time scale. The resonance at 3.02 ppm integrates to 12 protons and is assigned to all of the *p*-methyl groups on the aryl rings because these protons are far removed from the paramagnetic center and the inequivalency of the ligands. The three resonances that integrate to six protons each are assigned to the methyl groups on the backbone of the $^{Mes}DAB^{Me}$ ligand, the *o*-methyl groups that point parallel to the U−I bond on this ligand, and the *o*-methyl groups that point antiparallel along this bond for $^{Mes}DAB^{Me}$. For this ligand, the aryl CH protons are equivalent and assigned to the peak at 46.78 ppm integrating to four protons. The remaining resonances are assigned to $^{Mes}DAB^{Me2}$

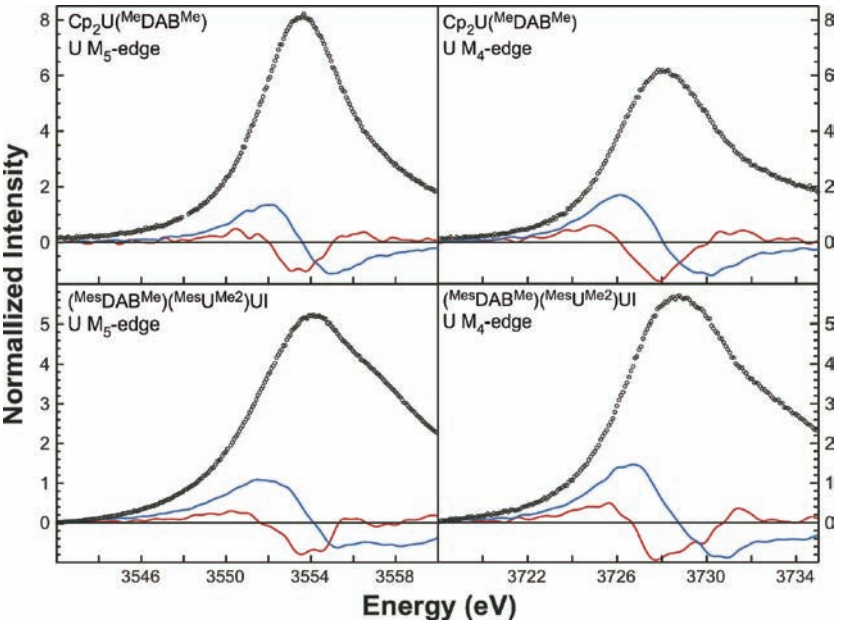

Figure 10. U M_5- (left) and M_4-edge (right) XANES data (○) for **2** (top) and **3** (bottom) overlaid on the first (blue line) and second (red line) derivatives of the data.

dx.doi.org/10.1021/ic2002805 |*Inorg. Chem.* 2011, 50, 9838–9848

because introduction of the additional methyl group from methyl iodide destroys the symmetry in the ligand. The three methyl groups on the ligand backbone are all inequivalent, as are the four *o*-methyl groups on the aryl rings; thus, these seven peaks integrate to three protons each. The remaining resonances at 6.85 and 7.35 ppm both have integration values for two protons, indicating equivalence, and are assigned to the *m*-CH in $^{Mes}DAB^{Me2}$.

In order to verify that complex **3** is best described as containing a tetravalent uranium ion, XANES measurements were made on **3** at the U M_5- and M_4-edges in comparison to analogous measurements on **2** (Figure 10). All spectra were calibrated in energy to the maximum of the first preedge feature of D_{2d}-Cs_2CuCl_4 (2820.20 eV). The M_5- and M_4-edge XANES spectra for **2** are quite similar to those for **3**, with the exception being the postedge regions (>3554 and >3730 eV for the M_5- and M_4-edge XANES spectra, respectively) for **3** containing more structure than that observed for **2**. The first and second derivative analyses show that the inflection points for the rising edges for **2** and **3** occur at similar energies. The U M_5-edge inflection points for **2** and **3** appear at 3551.58 and 3551.99 eV, respectively, and the U M_4-edge inflection points were determined to be at 3726.62 and 3726.13 eV, respectively. Given that the UV−vis/near-IR, variable-temperature magnetic susceptibility, and U L_{III}-edge XANES measurements all indicate that **2** contains a uranium(IV) $5f^2$ ion and because the U M_4- and M_5-edge XANES analyses show that the effective nuclear charge for **3** is quite similar to that of **2**, the overall analysis suggests that the uranium ion in **3** is of valence similar to that in **2** and is best described as containing U^{4+}.

The addition of iodomethane to produce **3** results in a multielectron reduction, whereby both the methyl group and the iodide come to rest on a mononuclear uranium species that has been confirmed to be tetravalent using XANES. This is significant because previous studies of iodomethane reduction have been demonstrated by a uranium(III) precursor to ultimately synthesize two new uranium(IV) products, one containing a new uranium−methyl moiety, and the other featuring a new uranium−iodide bond.[2,3,5] This reactivity occurs because one electron from each uranium center is donated to cleave the C−I bond. Utilizing the reduced ene-diamide framework creates an electron-rich uranium complex that can now perform the desired reaction on its own rather than bimolecularly. Transferring electrons to and from the system of the ligand enables two electron reductive HC_3-I bond cleavage. Since the valency of the metal does not change and the reduction chemistry originates from the ligand, overall this represents a new mode of chemistry observed for tetravalent uranium.

CONCLUSION

Uranium compounds, **1** and **2**, have been synthesized with the mesityl-substituted α-diimine ligand $^{Mes}DAB^{Me}$. The combined structural and spectroscopic studies presented here support both compounds as containing reduced ene-diamide ligands with uranium(IV) centers. This is further supported by magnetic measurements because both species show the characteristic temperature dependencies expected for tetravalent uranium centers despite the fact that their magnetic moments at room temperature are low compared to literature values. The addition of iodomethane to the bis(ligand) species **1** results in the activation and addition to the uranium complex, where the methyl group sits on the backbone of one of the enediamide ligands and the iodide becomes coordinated to uranium, forming **3**. In contrast, the cyclopentadienyl derivative **2** does not react with iodomethane, even at elevated temperatures.

The results reported herein highlight the use of redox-active ligands on uranium. Storing multiple electrons in the ligand framework gives the uranium(IV) complex the ability to perform multielectron activation of an alkyl halide. The chemistry presented here is in contrast to that previously observed, which requires reducing equivalents from two uranium centers for bond activation. Taking advantage of the redox activity of α-diimines with uranium facilitates multi-electron addition chemistry that has been previously unobserved at a single uranium complex.

ASSOCIATED CONTENT

Supporting Information. X-ray crystallographic data in CIF format, NMR spectra, spectra with peak labels, a table of peak shifts versus temperature, and additional X-ray crystallographic information. This material is available free of charge via the Internet at http://pubs.acs.org.

AUTHOR INFORMATION

Corresponding Author
*E-mail: sbart@purdue.edu.

ACKNOWLEDGMENT

We acknowledge the Petroleum Research Fund of the American Chemical Society (PRF 50460-DNI3) and Purdue University for financial support. S.C.B. acknowledges Benjamin Rogers for assistance with mass spectrometry measurements and Prof. Tong Ren for access to an electronic absorption spectrometer. E.J.S. acknowledges financial support from the University of Pennsylvania. E.J.S. and J.M.K. are grateful for partial support from the NSF MRSEC program under Award DMR-0520020. The XAS measurements were conducted at the SSRL, which is a national user facility supported by the U.S. Department of Energy (U.S. DOE), Office of Basic Energy Science. The XANES measurements were supported by a Glenn T. Seaborg Institute postdoctoral fellowship (S.R.D.) and the Division of Chemical Sciences, Geosciences, and Biosciences, Office of Basic Energy Sciences, U.S. DOE, under the Heavy Element Chemistry Program at Los Alamos National Laboratory. Los Alamos National Laboratory is operated by Los Alamos National Security, LLC, for the National Nuclear Security Administration of the U.S. Department of Energy under Contract DE-AC52-06NA25396.

REFERENCES

(1) Le Marechal, J. F.; Ephritikhine, M.; Folcher, G. *J. Organomet. Chem.* **1986**, *299*, 85.
(2) Finke, R. G.; Hirose, Y.; Gaughan, G. *J. Chem. Soc., Chem. Commun.* **1981**, 232.
(3) Finke, R. G.; Schiraldi, D. A.; Hirose, Y. *J. Am. Chem. Soc.* **1981**, *103*, 1875.
(4) Fagan, P. J.; Manriquez, J. M.; Marks, T. J.; Day, C. S.; Vollmer, S. H.; Day, V. W. *Organometallics* **1982**, *1*, 170.
(5) Villiers, C.; Ephritikhine, M. *J. Organomet. Chem.* **1990**, *393*, 339.
(6) Spencer, L. P.; Yang, P.; Scott, B. L.; Batista, E. R.; Boncella, J. M. *Inorg. Chem.* **2009**, *48*, 11615.

(7) Evans, W. J.; Montalvo, E.; Kozimor, S. A.; Miller, K. A. *J. Am. Chem. Soc.* **2008**, *130*, 12258.
(8) Evans, W. J.; Miller, K. A.; Kozimor, S. A.; Ziller, J. W.; DiPasquale, A. G.; Rheingold, A. L. *Organometallics* **2007**, *26*, 3568.
(9) Warner, B. P.; Scott, B. L.; Burns, C. J. *Angew. Chem., Int. Ed.* **1998**, *37*, 959.
(10) Bart, S. C.; Anthon, C.; Heinemann, F. W.; Bill, E.; Edelstein, N. M.; Meyer, K. *J. Am. Chem. Soc.* **2008**, *130*, 12536.
(11) Castro-Rodriguez, I.; Nakai, H.; Meyer, K. *Angew. Chem., Int. Ed.* **2006**, *45*, 2389.
(12) Castro-Rodriguez, I.; Olsen, K.; Gantzel, P.; Meyer, K. *J. Am. Chem. Soc.* **2003**, *125*, 4565.
(13) Budzelaar, P. H. M.; de Bruin, B.; Gal, A. W.; Wieghardt, K.; van Lenthe, J. H. *Inorg. Chem.* **2001**, *40*, 4649.
(14) De Bruin, B.; Bill, E.; Bothe, E.; Weyhermüller, T.; Wieghardt, K. *Inorg. Chem.* **2000**, *39*, 2936.
(15) Evans, W. J.; Kozimor, S. A. *Coord. Chem. Rev.* **2006**, *250*, 911.
(16) Diaconescu, P. L.; Cummins, C. C. *J. Am. Chem. Soc.* **2002**, *124*, 7660.
(17) Evans, W. J.; Nyce, G. W.; Ziller, J. W. *Angew. Chem., Int. Ed.* **2000**, *39*, 240.
(18) Evans, W. J.; Kozimor, S. A.; Ziller, J. W.; Kaltsoyannis, N. *J. Am. Chem. Soc.* **2004**, *126*, 14533.
(19) Diaconescu, P. L.; Arnold, P. L.; Baker, T. A.; Mindiola, D. J.; Cummins, C. C. *J. Am. Chem. Soc.* **2000**, *122*, 6108.
(20) Evans, W. J.; Kozimor, S. A.; Ziller, J. W. *Chem. Commun.* **2005**, 4681.
(21) Kraft, S. J.; Fanwick, P. E.; Bart, S. C. *Inorg. Chem.* **2010**, *49*, 1103.
(22) Kraft, S. J.; Walensky, J.; Fanwick, P. E.; Hall, M. B.; Bart, S. C. *Inorg. Chem.* **2010**, *49*, 7620.
(23) Bart, S. C.; Lobkovsky, E.; Chirik, P. J. *J. Am. Chem. Soc.* **2004**, *126*, 13794.
(24) Blackmore, K. J.; Ziller, J. W.; Heyduk, A. F. *Inorg. Chem.* **2005**, *44*, 5559.
(25) Bouwkamp, M. W.; Bowman, A. C.; Lobkovsky, E.; Chirik, P. J. *J. Am. Chem. Soc.* **2006**, *128*, 13340.
(26) Smith, A. L.; Hardcastle, K. I.; Soper, J. D. *J. Am. Chem. Soc.* **2010**, *132*, 14358.
(27) Zi, G.; Jia, L.; Werkema, E. L.; Walter, M. D.; Gottfriedsen, J. P.; Andersen, R. A. *Organometallics* **2005**, *24*, 4251.
(28) Korobkov, I.; Gorelsky, S.; Gambarotta, S. *J. Am. Chem. Soc.* **2009**, *131*, 10406.
(29) Schelter, E. J.; Wu, R.; Scott, B. L.; Thompson, J. D.; Cantat, T.; John, K. D.; Batista, E. R.; Morris, D. E.; Kiplinger, J. L. *Inorg. Chem.* **2010**, *49*, 924.
(30) Clark, D. L.; Sattelberger, A. P. *Inorg. Synth.* **1997**, *31*, 307.
(31) Chakraborty, S.; Chattopadhyay, J.; Guo, W.; Billups, W. E. *Angew. Chem., Int. Ed.* **2007**, *46*, 4486.
(32) Helmholz, L.; Kruh, R. F. *J. Am. Chem. Soc.* **1952**, *74*, 1176.
(33) Zhong, H. A.; Labinger, J. A.; Bercaw, J. E. *J. Am. Chem. Soc.* **2002**, *124*, 1378.
(34) Bradley, J. A.; Sen Gupta, S.; Seidler, G. T.; Moore, K. T.; Haverkort, M. W.; Sawatzky, G. A.; Conradson, S. D.; Clark, D. L.; Kozimor, S. A.; Boland, K. S. *Phys. Rev. B* **2010**, *81*, 193104/1.
(35) Kozimor, S. A.; Yang, P.; Batista, E. R.; Boland, K. S.; Burns, C. J.; Clark, D. L.; Conradson, S. D.; Martin, R. L.; Wilkerson, M. P.; Wolfsberg, L. E. *J. Am. Chem. Soc.* **2009**, *131*, 12125.
(36) Shadle, S. E. Ph.D. Thesis, Stanford University, Stanford, CA, 1994.
(37) Bain, G. A.; Berry, J. F. *J. Chem. Educ.* **2008**, *85*, 532.
(38) Sheldrick, G. M. *Acta Crystallogr.* **2008**, *112*, A64.
(39) Beurskens, P. T.; Beurskens, G.; de Gelder, R.; Garcia-Granda, S.; Gould, R. O.; Smits, J. M. M. *DIRDIF2008 Program System*; Crystallography Laboratory, University of Nijmegen: Nijmegen, The Netherlands, 2008.
(40) Cloke, F. G. N.; De Lemos, H. C.; Sameh, A. A. *J. Chem. Soc., Chem. Commun.* **1986**, 1344.
(41) Recknagel, A.; Noltemeyer, M.; Edelmann, F. T. *J. Organomet. Chem.* **1991**, *410*, 53.
(42) Massarweh, G.; Fischer, R. D. *J. Organomet. Chem.* **1993**, *444*, 67.
(43) Muresan, N.; Lu, C. C.; Ghosh, M.; Peters, J. C.; Abe, M.; Henling, L. M.; Weyhermüller, T.; Bill, E.; Wieghardt, K. *Inorg. Chem.* **2008**, *47*, 4579.
(44) Schaub, T.; Radius, U. *Z. Anorg. Allg. Chem.* **2006**, *632*, 807.
(45) Martins, R. S.; Filgueiras, C. L.; Visentin, L. d. C.; Bordinhao, J.; Ferreira, L. C. *Acta Crystallogr.* **2007**, *E63*, o4544.
(46) Gonsalvi, L.; Gaunt, J. A.; Adams, H.; Castro, A.; Sunley, G. J.; Haynes, A. *Organometallics* **2003**, *22*, 1047.
(47) Cope-Eatough, E. K.; Mair, F. S.; Pritchard, R. G.; Warren, J. E.; Woods, R. J. *Polyhedron* **2003**, *22*, 1447.
(48) Histogram from the Cambridge Crystallographic Database.
(49) Jantunen, K. C.; Burns, C. J.; Castro-Rodriguez, I.; Da Re, R. E.; Golden, J. T.; Morris, D. E.; Scott, B. L.; Taw, F. L.; Kiplinger, J. L. *Organometallics* **2004**, *23*, 4682.
(50) Summerscales, O. T.; Cloke, F. G. N.; Hitchcock, P. B.; Green, J. C.; Hazari, N. *Science* **2006**, *311*, 829.
(51) Marks, T. J. *Progress in Inorganic Chemistry*; John Wiley & Sons: New York, 1979; Vol. 25.
(52) Lam, O. P.; Anthon, C.; Heinemann, F. W.; O'Connor, J. M.; Meyer, K. *J. Am. Chem. Soc.* **2008**, *130*, 6567.
(53) Schelter, E. J.; Yang, P.; Scott, B. L.; Thompson, J. D.; Martin, R. L.; Hay, P. J.; Morris, D. E.; Kiplinger, J. L. *Inorg. Chem.* **2007**, *46*, 7477.
(54) Newell, B. S.; Rapp, A. K.; Shores, M. P. *Inorg. Chem.* **2010**, *49*, 1595.
(55) Kozimor Stosh, A.; Bartlett, B. M.; Rinehart, J. D.; Long, J. R. *J. Am. Chem. Soc.* **2007**, *129*, 10672.
(56) Fortier, S.; Melot, B. C.; Wu, G.; Hayton, T. W. *J. Am. Chem. Soc.* **2009**, *131*, 15512.
(57) Castro-Rodriguez, I.; Meyer, K. *Chem. Commun.* **2006**, 1353.
(58) Boudreaux, E. A.; Mulay, L. N. *Theory and Applications of Molecular Paramagnetism*; Wiley: New York, 1976; p 510.
(59) Liddle, S. T.; McMaster, J.; Mills, D. P.; Blake, A. J.; Jones, C.; Woodul, W. D. *Angew. Chem., Int. Ed.* **2009**, *48*, 1077.
(60) Bart, S. C.; Heinemann, F.; Anthon, C.; Hauser, C.; Meyer, K. *Inorg. Chem.* **2009**, *48*, 9419.
(61) Khusniyarov, M. M.; Bill, E.; Weyhermüller, T.; Bothe, E.; Harms, K.; Sundermeyer, J.; Wieghardt, K. *Chem.—Eur. J.* **2008**, *14*, 7608.